

OPEN

Flagellar Kinematics and Swimming of Algal Cells in Viscoelastic Fluids

SUBJECT AREAS:

FLUID DYNAMICS

MOTILITY

B. Qin¹, A. Gopinath^{1,2}, J. Yang^{1,2}, J. P. Gollub² & P. E. Arratia¹¹Department of Mechanical Engineering & Applied Mechanics, University of Pennsylvania, Philadelphia, PA 19104, ²Department of Physics & Astronomy, Haverford College, Haverford, PA 19041.Received
4 November 2014Accepted
23 February 2015Published
17 March 2015Correspondence and
requests for materials
should be addressed to
P.E.A. (parratia@seas.
upenn.edu)

The motility of microorganisms is influenced greatly by their hydrodynamic interactions with the fluidic environment they inhabit. We show by direct experimental observation of the bi-flagellated alga *Chlamydomonas reinhardtii* that fluid elasticity and viscosity strongly influence the beating pattern - the gait - and thereby control the propulsion speed. The beating frequency and the wave speed characterizing the cyclical bending are both enhanced by fluid elasticity. Despite these enhancements, the net swimming speed of the alga is hindered for fluids that are sufficiently elastic. The origin of this complex response lies in the interplay between the elasticity-induced changes in the spatial and temporal aspects of the flagellar cycle and the buildup and subsequent relaxation of elastic stresses during the power and recovery strokes.

The motility of microorganisms and organelles through microstructured fluids plays an important role in varied biological processes such as fertilization and genetic transport^{1–4}, development of disease⁵ and biodegradation in soil⁶. Disruption of normal motility can occur due to unexpected changes in the nature of the fluids. For instance, the graceful beating of filamentous cilia pumping mucus in the respiratory tract^{4,7,8} and the flagella driven swimming of spermatozoa through cervical mucus^{9,10} are both affected by the properties of the mucus such as water content and viscoelasticity. At larger scales, the undulatory motion of *Caenorhabditis elegans* in wet soil¹¹ or through polymer networks¹² is influenced by the rheology of the environment sensed by the worm as it moves. In addition, there is growing interest in designing artificial swimmers driven by external fields^{13,14} and developing objects capable of swimming remains a subject of intensive exploration.

Many organisms move in the realm of low Reynolds number $Re \equiv \ell / \nu \ll 1$ because of either small length scales ℓ , low swimming speeds U or both. In a Newtonian fluid with constant density ρ and viscosity η , this implies that inertial effects are negligible and that the stresses felt by the swimmer are purely viscous and linear in the viscosity. Since the Stokes equations govern the fluid response to the moving body, the fluid kinematics is reversible. To therefore swim, organisms must execute non-reversible, asymmetric strokes in order to break free of the constraints imposed by the so-called “scallop theorem”¹⁵. In many instances, however the ambient fluid environment is far from Newtonian due to the presence of macromolecules such as biopolymers and proteins, which impart complex rheological characteristics such as shear rate dependent viscosity and viscoelasticity. In a viscoelastic fluid, stresses are both viscous and elastic, and therefore time dependent - consequently, kinematic reversibility can break down. This effect is especially important for small organisms since the relaxation time of elastic stresses in the fluid λ may then become comparable to the viscous diffusion time of vorticity ℓ^2 / ν . For microorganisms with cyclical swimming strokes, the elastic stresses may then persist between periods and eventually dominate over viscous effects.

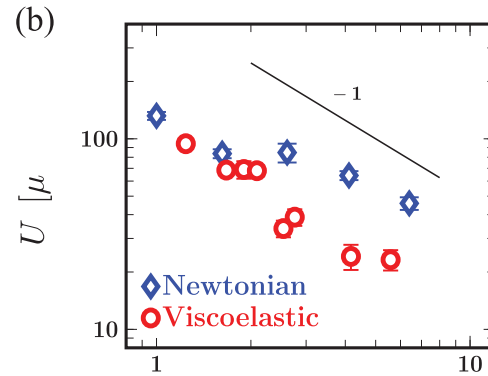
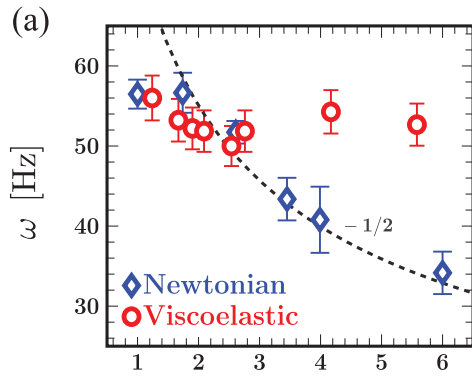
The consequences of fluid elasticity on the details of swimming while clearly important, are not well-understood, and have therefore received growing attention^{4,14,16–23}. Most recent work has been theoretical in nature relying on detailed simulations^{18,23,24} or asymptotic solutions to idealized models^{16,17,19}. Systematic experiments that may shed light are scarce and mainly focussed on swimming in Newtonian fluids^{25–27}. Taken together, current studies paint a complicated and sometimes contradictory picture. For instance, theories on the small amplitude swimming of infinitely long wave-like sheets suggest that elasticity can reduce swimming speed^{16,17} and these predictions are consistent with experimental observations of undulatory swimming in *C. elegans*²⁰. Similar trends were found recently²⁴ on studies of the motility of both idealized “pullers” (such as *Chlamydomonas reinhardtii*) and “pushers” (such as *Escherichia coli*). On the other hand, simulations of finite-sized moving¹⁸ filaments or large amplitude undulations²³ suggest that fluid elasticity can increase the propulsion speed - consistent this time with experiments on propulsion due to rotating rigid mechanical helices²². The emerging viewpoint is that fluid microstructure and swimming kinematics impact motility in a non-linear manner^{12,23}.

In this manuscript, we experimentally investigate the effects of fluid elasticity on the swimming behavior of the bi-flagella green alga, *Chlamydomonas reinhardtii*. With an ellipsoidal cell body (Fig. 1a) that is roughly 10 μm in size and two anterior flagella each of length $\ell \sim 10 \mu\text{m}$, the alga is a model system in biology²⁸ and has been widely used in studies on motility. The two flagella possess the same conserved “9 + 2” microtubule arrangement seen in other eukaryotic axonemes²⁸ and as a pair, execute cyclical breast-stroke like patterns with asymmetric power and recovery strokes at frequencies varying from $\sim 30\text{--}60$ Hz to generate propulsion^{27,28}. This swimming gait generates far-field flows corresponding to an idealized “puller”^{24,26}. By systematically modifying the elasticity of the fluid, we studied the variation of the flagellar beat pattern, beat frequency and centroid velocity. We find that fluid elasticity can modify the beating pattern (i.e. shape) and enhance the alga’s beating frequency and wave speed. Despite this enhancement, the alga’s swimming speed is overall hindered (as much as 50%) by fluid elasticity due to the elastic stresses in the fluid.

Two types of fluids are used – Newtonian and viscoelastic. Newtonian fluids are prepared by dissolving relatively small quantities of Ficoll (Sigma-Aldrich) in M1 buffer solution. The Ficoll concentration in M1 buffer is varied from 5% to 20% by weight in order

to produce fluids with a range of viscosities (1 cP to 10 cP). Viscoelastic fluids are prepared by adding small amounts of the flexible, high molecular weight polymer polyacrylamide (PAA, MW = 18×10^6 , Polysciences) to water. The polymer concentration in solution ranges from 5 to 80 ppm resulting in fluid relaxation times that range from 6 ms to 0.12 s, respectively (SI-§I, Figure 3a, Table 1). These polymeric solutions are considered dilute since the overlap concentration for PAA is approximately 350 ppm. All fluids are characterized using a cone-and-plate rheometer (RF3, TA Instruments); for more information, please see SI-§I. We use an effective viscosity $\eta_{\text{eff}} = [\eta(\dot{\gamma}_{\text{body}}) + \eta(\dot{\gamma}_{\text{flag}})]/2$ to study viscous effects on swimming in the polymeric fluids (Methods and Materials), where $\eta(\dot{\gamma})$ is the shear rate dependent viscosity. This enables us to compare swimming in these fluids to swimming in a Newtonian fluid with the same effective viscosity.

Dilute suspensions are made by suspending motile algae in either Newtonian (Ficoll) or viscoelastic (PAA) fluids. A small volume of this suspension is then stretched to form a thin film (thickness $\approx 20 \mu\text{m}$) using a wire-frame device (Methods and Materials, SI-§I, A), and cell motion in the thin film is imaged using an optical microscope and a high speed camera. The cell centroid and



flagella of cells that exhibited regular synchronous swimming strokes (for other observed gaits see SI-§II and SI-Movies) are identified and tracked. Figure 1(a) shows snapshots of *C. elegans* swimming at $Re \sim 10^{-3}$ in a water-like M1 buffer solution. The shapes of the flagella (red curves - Fig. 1a) as well as the trajectory of the cell centroid are tracked simultaneously with instantaneous swimming speeds calculated by differentiating the centroid position and the sign determined from the cell orientation. The speed of the swimmer measured in the thin liquid film set-up are consistent with that in the bulk fluid reported by other researchers²⁷.

The beating pattern of *C. elegans* over one cycle in Newtonian (N) and polymeric solutions (VE) of similar viscosity $\approx 6 \text{ mPa}\cdot\text{s}$ are presented in Fig. 1(b) (c.f. SI-§II for analogous shapes for $\approx 2.6 \text{ mPa}\cdot\text{s}$). The difference in shapes is striking and illustrates the effects of fluid elasticity on swimming. In the Newtonian case (i), the flagellum seems more mobile and significant changes in curvatures are attained over the whole cycle. In the viscoelastic case (ii), lateral displacements of almost a third of the flagellum close to the cell body (green) appear to be severely restricted (less mobile) or bundled together with most of the bending occurring over the remainder of the length. Furthermore, we observe localized bending at the distal tip in the initial stages of the power stroke. The differences in the shapes can be quantified by plotting the spatio-temporal evolution of the scaled flagellum curvature $\kappa(\ell, t) = \tilde{\kappa}(\ell, t) \cdot \ell$ over many cycles (Fig. 1c). These kymographs show that regions of high curvature are found to distribute diagonally and periodically, characteristic of propagating bending waves. In the elastic fluid, (Fig. 1c, right panel) flagella attain larger curvatures (dark blue regions) and an increase in the frequency of bending waves (diagonally oriented lines - direction shown by arrow). We also observed that for very low viscosities ($1 < \eta < 2.6 \text{ mPa}\cdot\text{s}$), the distal tip gets closer to the cell body than for higher viscosity fluids (SI, Fig. 7). We can quantify this difference in curvature by computing the normalized curvature averaged over time (≈ 6 cycles) and dimensionless arc length ℓ/ℓ , here denoted by $\langle \kappa \rangle$. We find that at $\approx 6 \text{ cP}$, the value of $\langle \kappa \rangle$ is -1.44 and -2.72 for the Newtonian and viscoelastic fluids, respectively.

These changes in the spatio-temporal dynamics of the flagella translate to variations in beat frequency and swimming speed. We begin by investigating the effects of shear viscosity on the beat frequency (Fig. 2a) and on the cycle averaged net swimming speed

(Fig. 2b). In Newtonian fluids, for viscosities $\sim 2 \text{ mPa}\cdot\text{s}$ and lower, the frequency is roughly around 56 Hz. Increasing the viscosity further ($> 2 \text{ mPa}\cdot\text{s}$) results in a monotonically decreasing frequency. Intriguingly, we find that the decay is well captured by $\sim 1/\sqrt{\eta}$ consistent with models suggesting that emergent frequencies are selected based on a balance of internal active processes, the elastic properties of the flagellum and external viscosity²⁹ (see also SI-§III). For polymeric fluids with low viscosities (low PAA concentration), the frequencies are consistent with the Newtonian values. At higher concentrations of polymer, however, significant deviation from the Newtonian trend is observed, even when the fluid has comparable viscosity. Surprisingly, the beating frequency increases with increasing fluid viscosity and then seems to saturate. Note from the data that the variation in beating frequencies at each characteristic fluid/relaxation time is small as seen from the relative size of the error bars compared to the mean value.

The observed increase in beating frequency, however, does not translate into an increase in overall swimming speed. Figure 2(b) shows that the average net swimming speed of the *C. elegans* cell body decreases as the fluid viscosity increases for both Newtonian and polymeric solutions. For low viscosity values ($< 2 \text{ mPa}\cdot\text{s}$), the swimming speeds are very similar for the algae cells in Newtonian and polymeric liquids. As polymer concentration increases, however, we find that fluid elasticity consistently hinders self-propulsion compared to Newtonian fluid at comparable viscosity. For both Newtonian and polymeric fluids, we find the data consistent with the relationship $U \sim \eta^{-1}$, which suggests that the algae are operating at nearly constant thrust. Such a relationship has also been observed for free swimming *C. elegans* in low viscosity Newtonian fluids ($1 < \eta < 2 \text{ mPa}\cdot\text{s}$)³⁰.

The data shown in Fig. 2 emphasize the increasing importance of elasticity as the polymer concentration in the fluid increases. Viscoelastic effects can be quantified by introducing the Deborah number, defined here as $De \equiv \omega \tau$ where ω is the mean frequency of a representative sample of cells and τ is the fluid relaxation time; we note that $De = 0$ for Newtonian fluids. The normalized beating frequency and algal swimming speed as a function of De are shown in Fig. 3(a) and 3(b), respectively. For ease of presentation, we normalize the measured frequency and net swimming speed with the Newtonian value at comparable viscosity. Figure 3(a) shows the

speed during the power stroke \bar{v}^+ and the mean speed during the recovery stroke \bar{v}^- for Newtonian and viscoelastic fluids. Figures 4(a) and 4(b) summarize our observations. For Newtonian fluids, both the power \bar{v}^+ and recovery \bar{v}^- stroke speeds decrease as ω increases, following the trend observed earlier for the Newtonian net swimming speed in Fig. 3(b). For viscoelastic fluids, however, we observe a sharp difference between power and recovery strokes. While the dependence of \bar{v}^+ is similar to the Newtonian case, the recovery speed \bar{v}^- in viscoelastic fluids remains relatively unchanged, and in fact modestly increases with viscosity. This raises the possibility that fluid elasticity affects power and recovery strokes very differently - a view supported by plots of the normalized power and recovery stroke speeds shown in Fig. 4(c) and 4(d). We observe a minimum in the values of $\bar{v}_E^+ / \bar{v}_N^+$ and $\bar{v}_E^- / \bar{v}_N^-$

monotonic increase in the frequency as the relaxation time of the fluid increases from around 20 to 120 ms. The transition from a Newtonian-like response ($De \lesssim 1$) to a clear viscoelastic regime occurs at around $De \sim 2.5$, where the frequency is on the order of the fluid relaxation time scale, suggesting that elastic fluid stresses are modifying kinematics. The ratio of swimming speeds plotted in Fig. 3(b) is consistently less than unity demonstrating that fluid elasticity hinders net locomotion. The decrease is quite substantial even for relatively low values of De . For example, fluid elasticity hinders the cell swimming speed, relative to Newtonian fluids, by as much as 50% for $De \approx 2$. We also observe that the ratio plateaus to approximately 0.4 for $De > 2$. This asymptotic behavior has been previously observed in theoretical studies^{16,17} and also in experiments with worms²⁰. The reduction in motility is also consistent with recent simulations²⁴ of steady flow of weakly elastic fluid around idealized pullers. This plateau may indicate an upper bound on the generated elastic stress around the organism.

The net frequency and swimming speed while central to the alga's overall motility, do not distinguish between the highly asymmetric power and recovery strokes. Therefore, we next calculate the mean





5. Celli, J. moves through mucus by reducing mucin viscoelasticity. **106**, 14321–14326 (2009).
6. Alexander, M. (R.E. Krieger, Malabar, FL, 1991).
7. Lillehoj, E. & Kim, K. Airway mucus: its components and function. **25**, 770–780 (2002).
8. Lai, S., Wang, Y., Wirtz, D. & Hanes, J. Micro- and macrorheology of mucus. **61**, 86–100 (2009).
9. Suarez, S. S. & Dai, X. Hyperactivation enhances mouse sperm capacity for penetrating viscoelastic media. **46**, 686–691 (1992).
10. Guzick, D. Sperm morphology, motility, and concentration in fertile and infertile men. **345**, 1388–1393 (2001).
11. Juarez, G., Lu, K., Sznitman, J. & Arratia, P. E. Motility of small nematodes in wet granular media. **92**, 44002 (2010).
12. Gagnon, D., Shen, X. & Arratia, P. Undulatory swimming in fluids with polymer networks. **104**, 14004 (2013).
13. Dreyfus, R. Microscopic artificial swimmers. **437**, 862 (2005).
14. Keim, N. C., Garcia, M. & Arratia, P. E. Fluid elasticity can enable propulsion at low Reynolds number. **24**, 081703 (2012).
15. Purcell, E. M. Lift at low Reynolds number. **45**, 3–11 (1977).
16. Fu, H. C., Wolgemuth, C. W. & Powers, T. R. Swimming speeds of filaments in nonlinearly viscoelastic fluids. **21**, 033102 (2009).
17. Lauga, E. Propulsion in a viscoelastic fluid. **19**, 083104–1–13 (2007).
18. Teran, J., Fauci, L. & Shelley, M. Fluid elasticity can enable propulsion at low Reynolds number. **104**, 038101 (2010).
19. Fu, H. C., Powers, T. R. & Wolgemuth, C. W. Theory of swimming filaments in viscoelastic media. **99**, 258101–1–4 (2007).
20. Shen, X. N. & Arratia, P. E. Undulatory swimming in viscoelastic fluids. **106**, 208101–1–4 (2011).
21. Pak, O. S., Zhu, L., Brandt, L. & Lauga, E. Micropropulsion and microrheology in complex fluids via symmetry breaking. **24**, 103102 (2012).
22. Liu, B., Powers, T. R. & Breuer, K. S. Force-free swimming of a model helical flagellum in viscoelastic fluids. **108**, 19516–19520 (2011).
23. Thomases, B. & Guy, R. D. Mechanisms of elastic enhancement and hindrance for finite length undulatory swimmers in viscoelastic fluids. **113**, 098102 (2014).
24. Zhu, L., Lauga, E. & Brandt, L. Self-propulsion in viscoelastic fluids: Pushers vs. pullers. **24**, 051902 (2012).
25. Berg, H. C. & Turner, L. Movement of microorganisms in viscous environments. **278**, 349–351 (1979).
26. Drescher, K., Goldstein, R., Michel, N., Polin, M. & Tuval, I. Direct measurement of the flow field around swimming microorganisms. **105**, 168101 (2010).
27. Guasto, J. S., Johnson, K. A. & Gollub, J. P. Oscillatory flows induced by microorganisms swimming in two dimensions. **105**, 168102 (2010).
28. Harris, E. H. (Academic Press, Oxford, 1999).
29. Camalet, S. & Julicher, F. Generic aspects of axonemal beating. **2**, 24.1–24.23 (2000).
30. Rafai, S., Jibuti, L. & Peyla, P. Effective viscosity of microswimmer suspensions. **104**, 098102 (2010).
31. Lauga, E. Life at high Deborah number. **86**, 64001–1–6 (2009).
32. Feng, J. & Leal, L. Transient extension and relaxation of a dilute polymer solution in a four-roll mill. **90**, 117–123 (2000).
33. Velez-Cordero, J. N. & Lauga, E. Waving transport and propulsion in a generalized Newtonian fluid. **199**, 37–50 (2013).
34. Gagnon, D., Keim, N. C. & Arratia, P. E. Undulatory swimming in shear-thinning fluids: experiments with **758**, R3 (2014).

Acknowledgments

We thank H. Hu, J. Guasto, G. Huber, X. Shen, N. Keim, D. Gagnon and A. Koser for insightful discussions, and K. Johnson for providing wild-type This work was supported by the National Science Foundation - DMR-1104705.

Author contributions

B.Q., J.Y., J.P.G. and P.E.A. designed experiments; J.Y. and B.Q. performed experiments; B.Q., A.G. and J.Y. analyzed experimental data; A.G., B.Q. and P.E.A. developed theories to interpret analysis; A.G., B.Q. and P.E.A. wrote the manuscript; all authors discussed and interpreted results; J.P.G. and P.E.A. conceived and supervised the project.

Additional information

Supplementary information accompanies this paper at <http://www.nature.com/scientificreports>

Competing financial interests: The authors declare no competing financial interests.

How to cite this article: Qin, B., Gopinath, A., Yang, J., Gollub, J.P. & Arratia, P.E. Flagellar Kinematics and Swimming of Algal Cells in Viscoelastic Fluids. **5**, 9190; DOI:10.1038/srep09190 (2015).



This work is licensed under a Creative Commons Attribution 4.0 International License. The images or other third party material in this article are included in the article's Creative Commons license, unless indicated otherwise in the credit line; if the material is not included under the Creative Commons license, users will need to obtain permission from the license holder in order to reproduce the material. To view a copy of this license, visit <http://creativecommons.org/licenses/by/4.0/>